Hydrothermal assisted synthesis of iron oxide-based magnetic silica spheres and their performance in magnetophoretic water purification

C. Caparrós[1], M. Benelmekki[1+,] P. Manuel[1], E. Xuriguera[2], C. J. Ribeiro Silva[3], Ll.M. Martinez[4], S. Lanceros-Méndez[1]

[1] *Centro de Física, Universidade do Minho, Campus de Gualtar, 4710-057 Braga, Portugal*

[2] *Facultat de Química, Universitat de Barcelona, 08028 Barcelona, Spain*

[3] *Departamento de Química, Universidade do Minho, Campus de Gualtar, 4710-057 Braga, Portugal*

[4] *Sepmag Technologies, Parc Tecnologic del Valles 08290 Barcelona, Spain*

Abstract

Porous Magnetic Silica (PMS) spheres of about 400 nm diameter were synthesised by one-pot process using the classical Stöber method combined with hydrothermal treatment. Cetyltrimethylammonium bromide (CTAB) was used as templating agent. The application of the hydrothermal process (120ºC during 48h) before the calcination leads to the formation of homogeneous and narrow size distribution porous magnetic silica spheres. This method allows to overcome the limitation of the formation of silica spheres without incorporation of magnetic particles. These achievements make this procedure interesting for industrial up scaling. The obtained PMS spheres were evaluated as adsorbents for Nickel cations in aqueous solution. In fact, 100% of the Ni^{2+} content was successfully removed from the aqueous solution without need to functionalize the silica surface.

1.- INTRODUCTION

The properties of materials with different morphologies and similar compositions. has become an important area of research and technological applications. In this way, the design of materials with controlled size, physical characteristics and morphology is gaining increasing attention (Calvert and Rieke 1996; Tanev et al. 1994). Some examples are hollow materials, nanoparticles, nanowires, nanotubes and many other unique structures (Lim et al. 2008; Lynch and Patrick 2002; Iijima 1991; Ryan et al. 2003; Hong et al. 2001; Zhu et al. 2004; Sohn et al. 2003; Sun and Xia 2002; Yin et al. 2004). The controlled synthesis of micro or nanoporous materials has been widely studied due to their potential application areas (Lu et al. 2007). Many synthesis methods for porous materials have been studied due to their interesting properties, such as high surface area, low density and large fractional void space properties (Gupta and Gupta 2005)

The encapsulation of magnetic nanoparticles inside silica spheres is becoming an important approach in the development of magnetic composites for bioapplications (Gao 2005; Chan 2007). Further, in the field of water purification, the use of the magnetic silica composites for the removing of metal ions from aqueous solutions is also being explored as the toxic heavy metal pollution is one of the most significant environmental problems(Girginova et al. 2010).

Porous morphologies can be achieved by using surfactants as templating agents (Brinker et al. 1999; Wang et al. 2005; Zeng et al. 2009; Zhang et al. 2010; Yuan et al. 2010). In general, there are four major methods for preparation of silica-coated magnetic nanoparticles: sol-gel, *in-situ* synthesis of nanoparticles together with the pre-synthesized silica nanoparticles, aerosol pyrolysis and water/oil emulsion method (Jolivet et al. 2004; Vestal and Zhang 2003). The sol–gel process has been widely studied and it consists in producing the silica phase on colloidal magnetic nanoparticles in a basic alcohol/water mixture (Van Ewijk et al. 1999). The production of size-controlled porous silica particles usually involves several separate synthetic steps (Querol et al. 2005). In general, separation or purification steps are required when multi-step reactions are performed (Taboada et al. 2009).

Despite the progress and the efforts to obtain optimum magnetic silica spheres, the current processing methods are not suitable for large volume production and therefore industrial applications due to their their high costs and low efficiency (low surface/volume ratio) (Chu 1999). Commercial magnetic silica composites are still under intensive research and are available only for research applications. In this way, the present work represents and attempt to overcome those limitations, contributing to the reduction of the production costs and improving the performance of the silica magnetic spheres.

For this purpose, Porous Magnetic Silica (PMS) spheres have been produced by a one-pot process using the classical Stöber method assisted by hydrothermal treatment. The cetyltrimethylammonium bromide (CTAB) surfactant is used as a templating agent. The combination of X-ray diffraction patterns (XRD), Infrared measurements (FTIR) and High Resolution Transmission Electron microscopy (HRTEM) was used to determine the composition and morphology of the obtained materials. The results show that the use of the hydrothermal treatment before the calcination process leads to the formation of homogeneous porous magnetic silica spheres. It is demonstrated that it is feasible to limit the formation of silica spheres without incorporation of magnetic particles. These achievements make this procedure interesting for industrial up scaling. Finally, the performance of the obtained PMS spheres was evaluated as an adsorbent for Nickel cations in aqueous solution.

2.- MATERIALS AND METHODS

Materials

The $FeSO_4 \cdot 7H_2O$ (CAS 7782-63-0), $FeCl_3 \cdot 6H_2O$ (CAS 10025-77-1), concentrated ammonium solution 28% (NH_4OH, CAS 1336-21-6), aitric acid monohydrate (CA, $C_6H_8O_7$, CAS 5949-29-1), tetraethyl ortosilicate (TEOS, $C_8H_{20}O_4Si$, CAS 78-10-4), cetyltrimethylammonium bromide (CTAB, $CH_3(CH_2)_{15}N(Br)(CH_3)_3$, CAS 57-09-0) and $NiCl_2 \cdot 6H_2O$ (CAS 7791-20-0) were obtained from Sigma-Aldrich.

Synthesis of magnetic nanoparticles

The synthesis of the magnetic nanoparticles were performed according to *Benelmekki et al*. (Benelmekki et al.). Nanoparticles were prepared by co-precipitation of ferrites from an aqueous mixture of $FeSO_4$ ($FeSO_4 \cdot 7H_2O$) and $FeCl_3$ ($FeCl_3$). NH_4OH was used as a precipitation agent. For this

purpose, $FeSO_4$ (0.67 M, 9.3 g in 50 mL) and $FeCl_3$ (1.27 M, 10.8 g in 50 mL) were mixed and heated to 80ºC. In order to precipitated the iron hydroxides, the pH value was raised and maintained to pH=10 for 30 min. The solution was rigorously stirred at a constant temperature during all the process. After an ageing time of 30 min, nanoparticles were magnetically separated and washed several times. Then, the pH value was increased to 10.5 - 11. The resultant solid magnetite material was dried in a vacuum oven at 60 °C for 24 h. Horizontal Low Gradient Magnetic Field (HLGMF) from Sepmag technologies was used for filtration, control and separation of synthesized magnetic nanoparticles.

Synthesis of the Porous Magnetic Silica(PMS) spheres:

Silica-coated magnetic NPs were prepared by the method of Stöber *et al*(Stöber et al. 1968). In a typical synthesis, 14 mL of aqueous solution of cetyltrimethylammonium bromide (CTAB) 0.8 wt% and 4.5 mL of ammonium solution were mixed with 60 mL of ethanol containing 15 mg of NPs at 25ºC. The concentration of the CTAB corresponds to 3.875 times the CTAB critical micelle concentration (CMC) (Modaressi et al. 2007). After ultrasonic vibration (35 kHz) for 5 min, 800 µL of tetraethyl orthosilicate (TEOS) was slowly added to the solution and maintained under ultrasonic vibration for 3 h and shaked for 21 h.

Two different procedures were followed depending on the synthetized particles ((Figure 1): i) The P1 samples was obtained by drying and resuspending the mixture in 10 mL of distilled water, being then transferred to a Teflon-lined stainless steel autoclave at 120ºC for 48 h. After the autoclave was cooled down to room temperature, the precipitate was separated by SEPMAG separator and washed with ethanol. ii) The sample P2 was prepared by calcination of the as-prepared sample at 400 °C for 8 h, followed by a hydrothermal treatment.

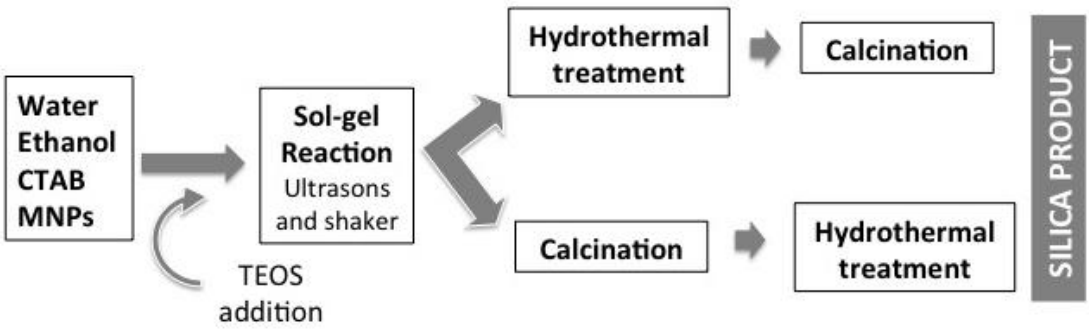

Figure 1. Schematic representation for the synthesis of silica products.

Adsorption of Ni^{2+} on the surface of the nanoparticles

In order to ensure experimental conditions, which promote the Ni^{2+} removal process, the ζ potential of the PMS spheres was studied. For this purpose, pH of the obtained PMS spheres was adjusted to different values, ranging from pH 3 to 11, with ammonia or clorhidric acid, maintaining the same ion concentration in all the suspensions.

For the removal of Ni^{2+} from an aqueous solution, 20 mg of the PMS spheres were mixed with 15 ml of nickel chloride aqueous solution at a concentration of 100 mg/L. The initial pH was settled to 9 using NH_3 0,1 M. The absorption experiment was performed at 150 rpm and room temperature. Five suspensions were prepared in the same conditions and each suspension was stirred during a fixed time. At the end of the stirring process, the PMS spheres were magnetically separated from the solution, and the sample solutions were filtered with a 0.200 μm pore filter. The final concentration of Ni^{2+} at each time interval was accessed by atomic absorption spectrometric method with flame atomization (AAS PYE Unicam SP9 - Philips).

Characterization methods

A LEO 906E electron microscope operating at 100 KeV was used for transmission electron microscopy characterization. The samples were prepared by deposition of a droplet of particles solution on a copper grid coated with carbon and allowed to dry.

Scanning electron microscopy (SEM) was performed in a JSM-6300 (*JEOL*) electron microscope operating at an accelerating voltage of 5 KeV. Dynamic light scattering (DLS) and ζ potential were performed with a Zetasizer Nano ZS (Malvern instruments), provided by a He/Ne laser of 633 nm wavelength. The NPs dispersion was analyzed in a polystyrene cell and in a folded capillary cell, for size distribution and zeta potential measurements, respectively. The ζ potential values were calculated using the Smoluchowski equation (Delgado et al. 2005). The obtained particles dried sample was characterized by X-ray diffraction with a Bruker D8 Discover diffractometer using Cu Kα incident radiation. Infrared measurements (FTIR) were performed at room temperature in a Perkin-

ElmerSpectrum apparatus in ATR mode from 4000 to 650 cm^{-1}. FTIR spectra were collected with 32 scans and a resolution of 4 cm^{-1}. The magnetophoresis setup employed in our experiment is the SEPMAG LAB 1x25 ml 2042 system (60T/m) (Sepmag Technologies, www.sepmag.eu). To determine the optimal magnetic separation times, precision magnetophoresis systems coupled to a backlight and a optical sensor were used. In the initial suspensions, particles are uniformly distributed and only a low amount of light is transmitted through it. Once the separation is completed and the magnetic beads are attached to the vessel wall, the suspension becomes transparent with a high increase in the light transmitted to the sensor. The variations of the transmitted light are used to determine when the magnetic separation is complete and therefore, to set the optimal times for the magnetophoretic separation.

3. RESULTS AND DISCUSSION

As shown in figure 2a, the peaks of the diffractogram corresponding to the synthesized nanoparticles can be indexed either to maghemite (γ-Fe_2O_3) or magnetite (Fe_3O_4). In order to simplify the nomenclatur, and considering the high probability of the oxidation of the Fe_3O_4 into γ-Fe_2O_3 (Laurent et al. 2008), the nomenclature was fixed on Fe_2O_3, instead of Fe_3O_4 and γ-Fe_2O_3. On the other hand, in the XRD pattern of the obtained P1 and P2 PMS spheres, the observed broaden peak at about 23º corresponds to the silica. This result confirms that the magnetic nanoparticles are well retained in the porous silica. No changes in the crystalline phase of the Fe_2O_3 nanoparticles were observed after the applied treatments. In figure 2b, the IR spectrums of the obtained PMS spheres show that CTAB was completely removed from the samples.

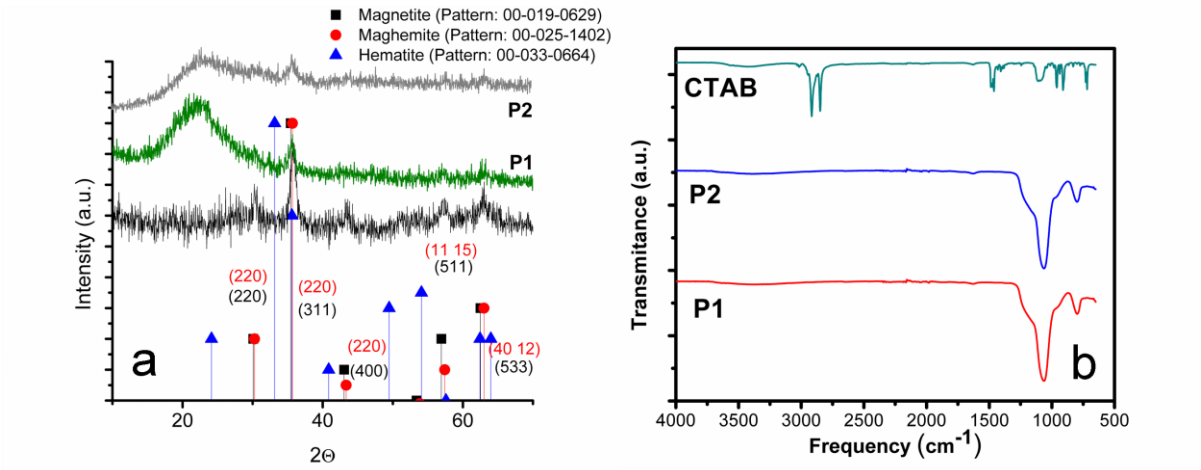

Figure 2. a) XRD pattern of the as-synthesized NPs (black) and P1 (Moeser et al.) and P2 (grey) PMS spheres . b) ATR-FTIR spectra of the synthesized P1 and P2 PMS spheres and the CTAB surfactant.

Figure 3 shows TEM and SEM images of the obtained P1 sample. The particles show a homogeneous "hollow-like" morphology and a spherical shape with a diameter of about 400 nm. The particles are porous with disordered pores. SEM image (figure 3C) shows also the "hollow-like" morphology of the obtained PMS spheres

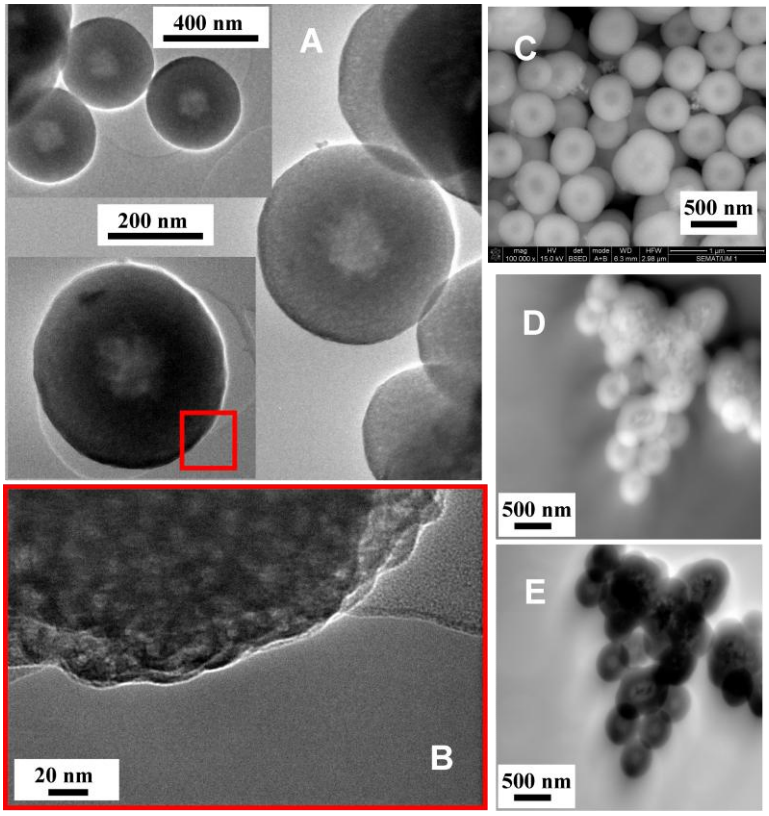

Figure 3. TEM (A, B) and SEM (C) images of sample P1 showing the "hollow-like" morphology of the obtained PMS spheres. (D, and (E) TEM images at bright and dark field modes.

Figure 4 shows the TEM images of the P2 particles, which were calcinated before the hydrothermal treatment. The obtained composites are the typical near spherical beads with Fe_2O_3 nanoparticles with a very large size distribution incorporated in the silica matrix. There is no evidence of the "hollow-like" morphology of the obtained PMS spheres. Moreover, it can be observed an important amount of spherical silica spheres with low incorporation of the Fe_2O_3 nanoparticles.

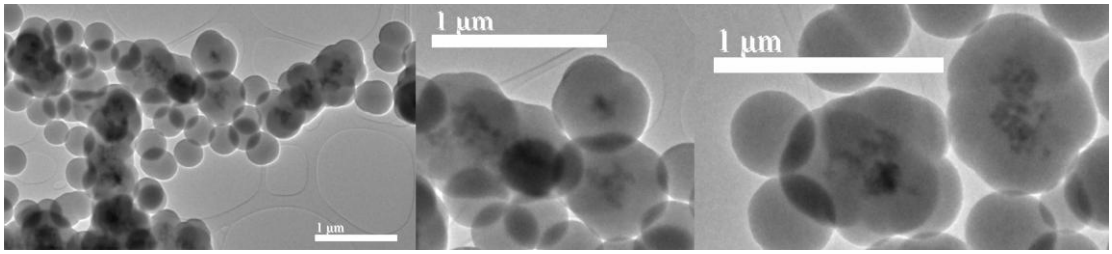

Figure 4. TEM images of the P2 sample showing the typical near spherical silica spheres with the incorporation of the Fe_2O_3 nanoparticles. An important amount of silica spheres with low incorporation of magnetic is also observed.

Figure 5 shows the magnetophoresis curves of the obtained P1 and P2 samples at 60 T/m magnetic field gradient. The sample concentrations were 5g/L. In the case of the P1 sample, the separation process takes about 16 min for the total separation of the particles. The observed behaviour is the typical of a magnetophoresis curve, consisting of a plateau corresponding to the reversible aggregation process of the particles followed by a progressive decay of the suspension opacity until 100% transparency is reached. In the case of the P2 sample, the magnetophoresis curve shows a first plateau followed by a week decay of the opacity and a second plateau followed by a progressive decay of the suspension opacity. This behavior suggests that the separation process occurs en two steps. The first magnetic separation takes about 16 min while the second separation process takes about 27 hours. Moreover, at the end of the magnethophoresis process of the P2 sample, the 100% transparency was not reached. This behavior is to be ascribed to the observed silica spheres without incorporation of magnetic particles that remain in suspension giving a white-opaque color suspension. These results are in agreement with TEM images in figure 4 showing the important amount of silica spheres without incorporation of magnetic nanoparticles. The total decay of the opacity of the P1 suspension is approximately 60% higher than the one for the P2 suspension.

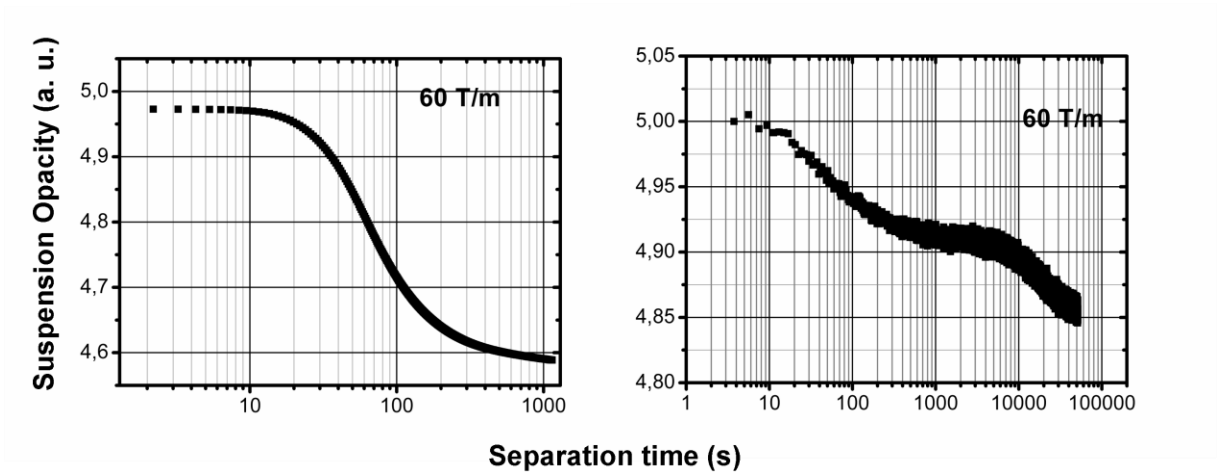

Figure 5 Magnetophoresis behaviour of the P1 and P2 samples at 60 T/m magnetic field gradient.

The mechanism of formation of PMS spheres can be explained by adjusting the synthesis parameters, which includes: i) The kinetics of the reaction (hydrolysis and condensation), ii) The interaction between the Fe_2O_3 nanoclusters and nanoparticles the CTAB micelles and individual molecules, and iii) The interaction between the CTAB and the silica. In the initial point of our experimental procedure, CTAB and Fe_2O_3 nanoparticles and nanoclusters are present in the ethanol-water mixture and the pH is maintained at 10. The electrostatic interaction between the specimens present in the suspension might be the driving force for the required organization of the suspension: Fe_2O_3 nanoparticles and nanoclusters are negatively charged whereas the CTAB micelles are positively charged. This interaction will lead to the formation of different combinations between the different specimens in the suspension (Figure 6).

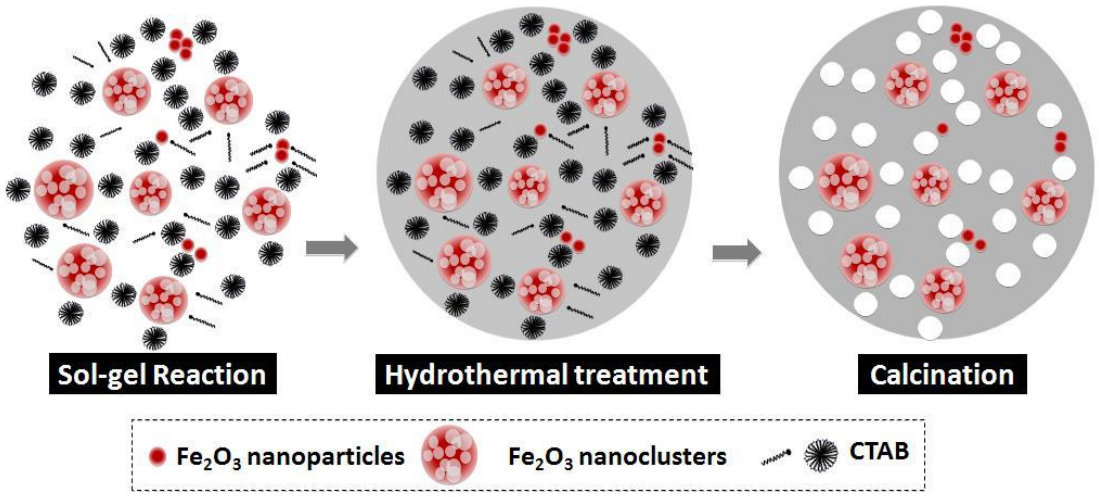

Figure 6. Formation mechanism of Porous Magnetic Silica (PMS) spheres.

When TEOS is added to the reaction mixture, the initial hydrolyzed products are growing around the CTAB-silica interface during the silicate polymerization process (Hayes et al. 1988; Edler and White 1997). The repeated growing process would create a highly branched network with interconnected channels (Tao and Li 2005). When basic pH is used, the positively charged heads of the templating self-assembled surfactants, S^+, interacts with the negative silica, I^-, controlling the surface-inorganic

interface which relies on the $\{S^+, I^-\}$ pathway by electrostatic forces (Xu et al. 2007). During the hydrolysis process, the formation of droplets containing silicate, CTAB, Fe_2O_3.-nanoclusters, ethanol and water can be generated in the PMS spheres (Zheng et al. 2007). The use of the hydrothermal treatment will remove the ethanol-water solvent trapped inside the gel pores, after the gel is formed by hydrolysis and condensation of a silicon precursor (Cabella et al. 2006). This treatment will help to the distribution of Fe_2O_3-nanoclusters and nanoparticles uniformly in to the volume of the silica spheres.

In the calcination process, the silica shell of the P1 particles is slightly strong to maintain the surface tension of the capillary force during the drying process. During the calcinating process CTAB contained in the shell is removed. The thermal treatment at 400ºC does not cause the recombination of Si-O-Si bonds, neither the destruction of the wall structure.

The comparison of P1 and P2 samples allows an overview of the role of the hydrothermal treatment on the formation mechanism of PMS spheres with hollow-like morphology. In the case of P1 samples, silica condenses on the external surface, thereby forming the interior which contains the agglomerated surfactant and/or the Fe_2O_3-nanoclusters (Li et al. 2003). Moreover, under the pressure induced by the hydrothermal treatment, the remaining free-silica magnetic nanoparticles in the suspension are incorporated to the silica spheres. Subsequent calcination leads to the formation of PMS spheres containing magnetic nanoclusters and nanoparticles dispersed in all the silica spheres (Lee et al. 2007). This behaviour explains the strong contrast between the dark edge and the pale centre in the TEM and SEM images of the PMS spheres (Figures 3) leading to a hollow-like morphology. On the other hand, TEM images of the PMS spheres at bright and dark field modes (figures 3D and 3E) show again the strong contrast between the bright edge and the pale centre and the dark edge and the pale centre, respectively including the case of the incorporation of the magnetic clusters in the centre of the silica. These results confirm that the obtained PMS spheres are not hollow. In the case of P2 samples the obtained morphology is undefined-hollow-like.

PMS spheres removing performance of Ni^{2+} using P1 and P2 PMS spheres

Negative values of the ζ potential of the synthesized PMS spheres in the stable suspension were used as a criterion for the efficiency of the removing process. As mentioned before, the evolution of ζ potential

of the obtained PMS spheres is determined as a function of the pH suspension (Figure 7). The results of the electrophoresis measurements show a highly negative ζ potential of the P1 and P2 samples for pH suspensions with values superiors to 7.

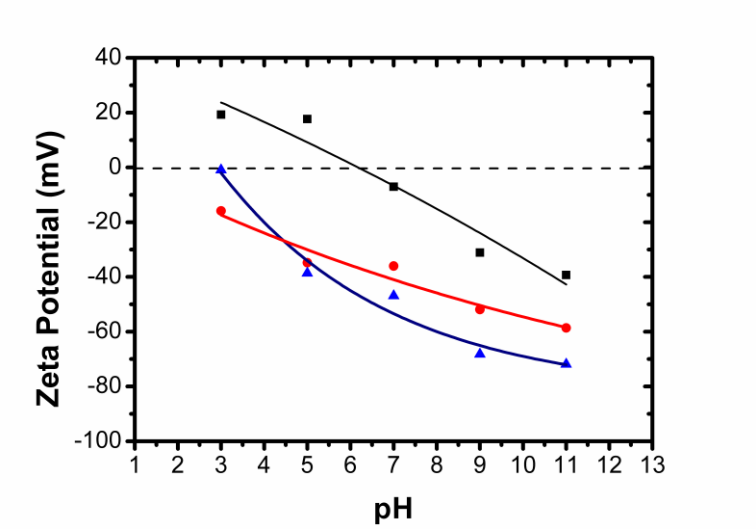

Figure 7. ζ potential behavior of P1 (Triangle), P2 (Circle), and the as synthesized Fe_2O_3 nanoparticles versus the pH of the different suspensions.

Considering the electrophoresis results in order to remove the Ni^{2+} ions from the aqueous solution, the initial pH was settled to 9, where P1 and P2 samples show ζ potential values of about -67 and -51 mV, respectively. The results of the nickel adsorption evolution as a function of the time treatment are shown in figure 8. The obtained curves show that in the case of P1 sample, the total amount of Ni^{2+} was removed from the solution at a maximum time of 3 hours. The time behavior suggests that a process of adsorption-desorption has occurred between 15 and 60 min. In the case of the P2 sample the curve shows also an adsorption-desorption process in the 5-15 min time interval. However, the total removing of the Ni^{2+} ions was not achieved in this case. An amount of about 15 ppm remains in the analyzed solution.

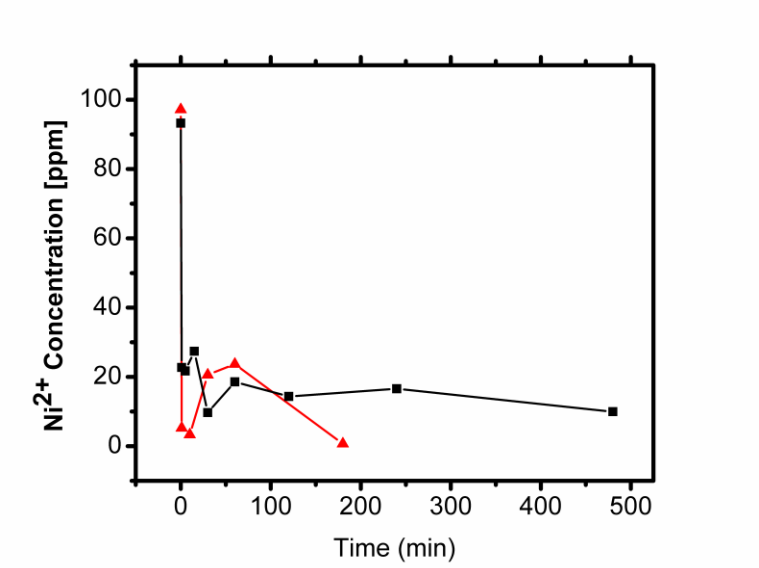

Figure 8. Evolution of the Ni^{2+} concentration in the aqueous solution. P1 (Triangle), P2 (Square).

Both P1 and P2 samples allow removing the Ni^{2+} ions from aqueous solutions, in agreement with the fact that silica surfaces are claimed to act as adsorbents for cationic species (Girginova et al. 2010; Huang and Chen 2009; Kursunlu et al. 2009). Moreover, it was verified the effect of –OH and $–NH_2$ terminals involved in the adsorption process and Ni^{2+} removed amounts of 18.6% and 100% using –OH and $–NH_2$ terminals, respectively, and 12.8% in the case of non-functionalized magnetic nanoparticles Girginova et al. (2010). In this context, Modaressi *et al.* (2007) reported that the Hg^{2+} removing capacity of no functionalized silica is limited to 24%.

The apparent rugosity of the surface of the particles will help to enhance the equilibrium level, where a saturation point is reached. The specific surface area of the PMS spheres (P1) is then responsible for the complete removal of the Ni^{2+} ions from water, being required for the stabilization of the Ni^{2+} adsorption.

4.- CONCLUSIONS

Porous, homogeneous and narrow size distribution of Magnetic Silica (PMS) spheres are generated by one-pot process using the classical Stöber method combined with hydrothermal treatment. It is demonstrated that it is possible to overcome the limitation of the formation of silica spheres without incorporation of magnetic particles by the use of hydrothermal treatment before the calcination process.

PMS spheres obtained by this procedure allow removing 100% Ni^{2+} content from an aqueous solution, without need to functionalize the silica surface. PMS spheres obtained by the calcination process before the hydrothermal treatment, attain the equilibrium conditions when 85% of the adsorption of Ni^{2+} is reached.

These achievements will contribute to the optimization of magnetic silica spheres production processes making them cost effective for industrial production. Moreover, the obtained morphology by the presented procedure make the PMS spheres an interesting tool for capturing and purification of bio-specimens based on the metal affinity adsorption.

Acknowledgements

This work is funded by FEDER funds through the "Programa Operacional Factores de Competitividade – COMPETE" and by national funds by FCT- Fundação para a Ciência e a Tecnologia, project references PTDC/CTM/69316/2006, and NANO/NMed-SD/0156/2007. The authors also thank support from the COST Action MP1003, 2010 'European Scientific Network for Artificial Muscles'. M.B. thank the FCT for support under the "*Compromisso com a Ciência*" program.

REFERENCES

Benelmekki M, Caparros C, Montras A, Gonçalves R, Lanceros-Mendez S, Martinez LM Horizontal low gradient magnetophoresis behaviour of iron oxide nanoclusters at the different steps of the synthesis route. Journal of Nanoparticle Research:1-8

Brinker CJ, Lu Y, Sellinger A, Fan H (1999) Evaporation-induced self-assembly: nanostructures made easy. Advanced Materials 11 (7):579-585

Cabella C, Crich SG, Corpillo D, Barge A, Ghirelli C, Bruno E, Lorusso V, Uggeri F, Aime S (2006) Cellular labeling with Gd (III) chelates: only high thermodynamic stabilities prevent the cells acting as ëspongesí of Gd3+ ions. Contrast media & molecular imaging 1 (1):23-29

Calvert P, Rieke P (1996) Biomimetic mineralization in and on polymers. Chemistry of Materials 8 (8):1715-1727

Chan WCW (2007) Bio-applications of Nanoparticles, vol 620. Springer Verlag,

Chu B (1999) Controlled size polymeric microspheres with superparamagnetic core, WO 99/12000, PCT/US98/21266.

Delgado A, Gonzalez-Caballero F, Hunter R, Koopal L, Lyklema J (2005) Measurement and interpretation of electrokinetic phenomena. Pure Appl Chem 77 (10):1753-1805

Edler K, White J (1997) Further improvements in the long-range order of MCM-41 materials. Chemistry of Materials 9 (5):1226-1233

Gao Y (2005) Biofunctionalization of magnetic nanoparticles.

Girginova PI, Daniel-da-Silva AL, Lopes CB, Figueira P, Otero M, Amaral VS, Pereira E, Trindade T (2010) Silica coated magnetite particles for magnetic removal of Hg2+ from water. Journal of Colloid and Interface Science 345 (2):234-240

Gupta AK, Gupta M (2005) Synthesis and surface engineering of iron oxide nanoparticles for biomedical applications. Biomaterials 26 (18):3995-4021

Hayes KF, Papelis C, Leckie JO (1988) Modeling ionic strength effects on anion adsorption at hydrous oxide/solution interfaces. Journal of Colloid and Interface Science 125 (2):717-726

Hong BH, Bae SC, Lee CW, Jeong S, Kim KS (2001) Ultrathin single-crystalline silver nanowire arrays formed in an ambient solution phase. Science 294 (5541):348

Huang SH, Chen DH (2009) Rapid removal of heavy metal cations and anions from aqueous solutions by an amino-functionalized magnetic nano-adsorbent. Journal of hazardous materials 163 (1):174-179

Iijima S (1991) Helical microtubules of graphitic carbon. Nature 354 (6348):56-58

Jolivet JP, Chanéac C, Tronc E (2004) Iron oxide chemistry. From molecular clusters to extended solid networks. Chem Commun (5):477-483

Kursunlu AN, Guler E, Dumrul H, Kocyigit O, Gubbuk IH (2009) Chemical modification of silica gel with synthesized new Schiff base derivatives and sorption studies of cobalt (II) and nickel (II). Applied Surface Science 255 (21):8798-8803

Laurent S, Forge D, Port M, Roch A, Robic C, Vander Elst L, Muller RN (2008) Magnetic Iron Oxide Nanoparticles: Synthesis, Stabilization, Vectorization, Physicochemical Characterizations, and Biological Applications. Chemical Reviews 108 (6):2064-2110. doi:10.1021/cr068445e

Lee DW, Park SJ, Ihm SK, Lee KH (2007) One-pot synthesis of Pt-nanoparticle-embedded mesoporous titania/silica and its remarkable thermal stability. The Journal of Physical Chemistry C 111 (21):7634-7638

Li, Shi, Hua, Chen, Ruan, Yan (2003) Hollow Spheres of Mesoporous Aluminosilicate with a Three-Dimensional Pore Network and Extraordinarily High Hydrothermal Stability. Nano Letters 3 (5):609-612. doi:10.1021/nl034134x

Lim JA, Lee WH, Lee HS, Lee JH, Park YD, Cho K (2008) Self Organization of Ink jet Printed Triisopropylsilylethynyl Pentacene via Evaporation Induced Flows in a Drying Droplet. Advanced Functional Materials 18 (2):229-234

Lu AH, Salabas EL, Sch¸th F (2007) Magnetic nanoparticles: synthesis, protection, functionalization, and application. Angewandte Chemie International Edition 46 (8):1222-1244

Lynch MD, Patrick DL (2002) Organizing carbon nanotubes with liquid crystals. Nano Letters 2 (11):1197-1201

Modaressi A, Sifaoui H, Grzesiak B, Solimando R, Domanska U, Rogalski M (2007) CTAB aggregation in aqueous solutions of ammonium based ionic liquids; conductimetric studies. Colloids and Surfaces A: Physicochemical and Engineering Aspects 296 (1-3):104-108

Moeser G, Green W, Laibinis P, Linse P, Hatton T (2004) Structure of polymer-stabilized magnetic fluids: Small-angle neutron scattering and mean-field lattice modeling. Langmuir 20 (13):5223-5234

Querol M, Chen JW, Weissleder R, Bogdanov Jr A (2005) DTPA-bisamide-based MR sensor agents for peroxidase imaging. Organic letters 7 (9):1719-1722

Ryan KM, Erts D, Olin H, Morris MA, Holmes JD (2003) Three dimensional architectures of ultra-high density semiconducting nanowires deposited on chip. Journal of the American Chemical Society 125 (20):6284-6288

Sohn BH, Choi JM, Yoo SI, Yun SH, Zin WC, Jung JC, Kanehara M, Hirata T, Teranishi T (2003) Directed self-assembly of two kinds of nanoparticles utilizing monolayer films of diblock copolymer micelles. Journal of the American Chemical Society 125 (21):6368-6369

Stöber W, Fink A, Bohn E (1968) Controlled growth of monodisperse silica spheres in the micron size range. Journal of Colloid and Interface Science 26 (1):62-69

Sun Y, Xia Y (2002) Shape-controlled synthesis of gold and silver nanoparticles. Science 298 (5601):2176

Taboada E, Solanas R, RodrÌguez E, Weissleder R, Roig A (2009) Supercritical Fluid Assisted One Pot Synthesis of Biocompatible Core (Fe2O3)/Shell (SiO2) Nanoparticles as High Relaxivity T2 Contrast Agents for Magnetic Resonance Imaging. Advanced Functional Materials 19 (14):2319-2324

Tanev PT, Chibwe M, Pinnavaia TJ (1994) Titanium-containing mesoporous molecular sieves for catalytic oxidation of aromatic compounds.

Tao C, Li J (2005) Morphosynthesis of microskeletal silica spheres templated by W/O microemulsion. Colloids and Surfaces A: Physicochemical and Engineering Aspects 256 (1):57-60

Van Ewijk G, Vroege G, Philipse A (1999) Convenient preparation methods for magnetic colloids. Journal of Magnetism and Magnetic Materials 201 (1-3):31-33

Vestal CR, Zhang ZJ (2003) Synthesis and magnetic characterization of Mn and Co spinel ferrite-silica nanoparticles with tunable magnetic core. Nano Letters 3 (12):1739-1743

Wang X, Zhuang J, Peng Q, Li Y (2005) A general strategy for nanocrystal synthesis. Nature 437 (7055):121-124

Xu R, Pang W, Yu J (2007) Chemistry of zeolites and related porous materials: synthesis and structure. Wiley-Interscience,

Yin Y, Rioux RM, Erdonmez CK, Hughes S, Somorjai GA, Alivisatos AP (2004) Formation of hollow nanocrystals through the nanoscale Kirkendall effect. Science 304 (5671):711

Yuan J, Zhang X, Qian H (2010) A novel approach to fabrication of superparamagnetite hollow silica/magnetic composite spheres. Journal of Magnetism and Magnetic Materials 322 (15):2172-2176

Zeng W, Xu H, Yang Y, Gu H (2009) Relationship between surface structure and morphology of Fe3O4/silica composite nanospheres and nucleic acid extraction. Journal of Magnetism and Magnetic Materials 321 (10):1485-1489

Zhang G, Liao Y, Baker I (2010) Surface engineering of core/shell iron/iron oxide nanoparticles from microemulsions for hyperthermia. Materials Science and Engineering: C 30 (1):92-97

Zheng T, Pang J, Tan G, He J, McPherson GL, Lu Y, John VT, Zhan J (2007) Surfactant Templating Effects on the Encapsulation of Iron Oxide Nanoparticles within Silica Microspheres. Langmuir 23 (9):5143-5147. doi:10.1021/la063761+

Zhu MQ, Wang LQ, Exarhos GJ, Li ADQ (2004) Thermosensitive gold nanoparticles. Journal of the American Chemical Society 126 (9):2656-2657